

Two Series of Novel Rare Earth Complexes with Dicyanamide [Ln(dca)₂(phen)₂(H₂O)₃][dca]·(phen), (Ln = Pr, Gd, and Sm) and [Ln(dca)₃(2,2'-bipy)₂(H₂O)]_n, (Ln = Gd, Sm, and La): Syntheses, Crystal Structures, and Magnetic Properties

A-Qing Wu,^{†,‡} Fa-Kun Zheng,[†] Wen-Tong Chen,[†] Li-Zhen Cai,[†] Guo-Cong Guo,^{*,†} Jin-Shun Huang,[†] Zhen-Chao Dong,[§] and Yoshihiko Takano[§]

State Key Laboratory of Structural Chemistry, Fujian Institute of Research on the Structure of Matter, The Chinese Academy of Sciences, Fuzhou, Fujian 350002, People's Republic of China, Graduate School, The Chinese Academy of Sciences, Beijing 100039, People's Republic of China, and National Institute for Materials Science, 1-2-1 Sengen, Tsukuba, Ibaraki 305-0047, Japan

Received December 20, 2003

Two series of novel complexes, [Ln(dca)₂(Phen)₂(H₂O)₃](dca)·(phen) (Ln = Pr (1), Gd (2), and Sm (3), dca = N(CN)⁻, phen = 1,10-phenanthroline) and [Ln(dca)₃(2,2'-bipy)₂(H₂O)]_n, (Ln = Gd (4), Sm (5), and La (6), 2,2'-bipy = 2,2'-bipyridine), have been synthesized and structurally characterized by X-ray crystallography. The crystal structures of the first series (1–3) are isomorphous and consist of discrete [Ln(dca)₂(Phen)₂(H₂O)₃]⁺ cations, dca anions, and lattice phen molecules; whereas the structures of the second series (4–6) are characterized by infinite chains [Ln(dca)₃(2,2'-bipy)₂(H₂O)]_n. The Ln(III) atoms in all complexes are nine-coordinated and form a distorted tricapped trigonal prism environment. The three-dimensional frameworks of 1–6 are constructed by intermolecular hydrogen bond interactions. Variable-temperature magnetic susceptibility measurements for complexes 1, 2, 4, and 5 indicate a Curie–Weiss paramagnetic behavior over 5–300 K.

Introduction

Paramagnetic centers have been found to be able to interact through extended bridging ligands, even if these centers are relatively far away from each other.¹ A number of molecule-based magnetic materials have been found to consist of paramagnetic metal ions and organic species. The metal ions are the sources of magnetic moments while the organic species provide super-exchange pathways between the magnetic centers. A change in the metal ions and/or super-exchange pathways produces a modification of crystal structure, which in turn may affect the magnetic ground state.² In 1993 Kahn advanced the Kanamori–Goodenough rules to give an explanation for the occurrence of ferro- or antiferromagnetic exchange for d-block elements.³ However,

to date, such effect has not yet been demonstrated for f-elements. Super-exchange is relatively unimportant for the rare earth ions due to the 4f electrons being well-shielded by the outer shells of 5s and 5p orbits and thus barely involved in chemical bonding. The conventional magnetic coupling between magnetic ions directly or via magnetic ions–ligand–magnetic ions does not work anymore for lanthanide complexes. It is the magnetic dipole–dipole interaction that decides the magnetic properties of most rare earth complexes. But rare earth ions generally have large anisotropic magnetic moment arising from a large number of spins and strong spin–orbit coupling so that *J*, rather than *S*, is an important quantity for magnetic properties.

On the other hand, dicyanamide is a versatile ligand with three nitrogen donor atoms; it may act as a uni-, bi-, and tridentate ligand.⁴ The varieties of its coordination modes allow for the preparation of complexes with a large variety of architectures, both mononuclear and multinuclear as well

* Author to whom correspondence should be addressed. E-mail: gcguo@ms.fjirsm.ac.cn.

[†] Fujian Institute of Research on the Structure of Matter, The Chinese Academy of Sciences.

[‡] Graduate School, The Chinese Academy of Sciences.

[§] National Institute for Materials Science.

(1) Gatteschi, D.; Bencini, A.; D.; Bencini, A. In *Magneto-Structural Correlations in Exchange Coupled Systems*; Willett, R. D., Gatteschi, D., Kahn, O., Eds.; Reidel: Dordrecht, 1985; p 241.

(2) Kmety, C. R.; Huang, Q. Z.; Lynn, J. W.; Erwin, R. W.; Manson, J. L.; McCall, S.; Crow, J. E.; Stevenson, K. L.; Miller, J. S.; Epstein, A. *J. Phys. Rev. B* **2000**, *62*, 5576.

(3) Kahn, O. *Molecular Magnetism*; VCH: New York, 1993.

as one-, two-, and three-dimensional networks. The complexes formulated as $[M(\text{dca})_2]_n$ ($M = \text{Mn, Fe, Co, Ni, Cu, Zn, Ag, etc.}$) containing only dca ligands have been synthesized,⁵ which revealed a very rich variety of topologies and magnetic properties; those for Co ($T_c = 9$ K) and Ni ($T_c = 20$ K) behaved as ferromagnets while for Cr ($T_N = 47$ K), Mn ($T_N = 16$ K), and Fe ($T_N = 19$ K) spin-canted antiferromagnets were reported.^{5c,e} The complexes with general formula $[M(\text{L})_x(\text{dca})_y]_z$ ($M = \text{Mn, Fe, Co, Ni, Cu, Zn; L = organic ligand; } x = 1 \text{ or } 2, y = 2, z = 1$) have been synthesized by using ancillary ligands such as pyrazine, pyridine, bipyridine, pyrimidine, bipyrimidine, 1,10-phenanthroline, etc. in addition to the dca ligand.^{4b,5d,6} In all these metal complexes, the metal atoms are almost the first row transition metals while rare earth metal atoms are quite rare; the only known example being $\text{Nd}(\text{P}(\text{MeN})_3)_2(\text{dca})_3$.⁷ To explore further dca-bridged metal complexes,⁸ we report here the syntheses and structures of six novel complexes containing rare earth and dca ligand, $[\text{Ln}(\text{dca})_2(\text{Phen})_2(\text{H}_2\text{O})_3](\text{dca})\cdot(\text{phen})$, where Ln = Pr (**1**), Gd (**2**), and Sm (**3**), and

$[\text{Ln}(\text{dca})_3(2,2'\text{-bipy})_2(\text{H}_2\text{O})]_n$, where Ln = Gd (**4**), Sm (**5**), and La (**6**), as well as the magnetic properties of complexes **1, 2, 4, and 5**.

Experimental Section

Materials and Measurement. All reagents except for $\text{LnCl}_3\cdot 6\text{H}_2\text{O}$ and $\text{Ln}(\text{ClO}_4)_3$ were commercial grade materials and used as received. $\text{Na}(\text{dca})$ was purchased from Aldrich Company. $\text{LnCl}_3\cdot 6\text{H}_2\text{O}$ and $\text{Ln}(\text{ClO}_4)_3$ were prepared by the reactions of Ln_2O_3 and hydrochloric acid or perchloric acid in aqueous solution. Elemental analyses (C, H, N) were determined on an Elementar Vario ELIII analyzer. IR spectra were measured as KBr pellets on a Nicolet Magna 750 FT IR spectrometer in the range of 400–4000 cm^{-1} . Magnetic susceptibilities of complexes **1, 2, 4, and 5** were measured by using a Quantum Design SQUID magnetometer in the temperature range 5–300 K at a field of 1 T. The raw data were corrected for the magnetization of the sample holder.

Preparations of $[\text{Ln}(\text{dca})_2(\text{Phen})_2(\text{H}_2\text{O})_3](\text{dca})\cdot(\text{phen})$ (1–3**).** A mixture of reactants was obtained by adding $\text{LnCl}_3\cdot 6\text{H}_2\text{O}$ (0.5 mmol) in 0.5 mL of H_2O and $\text{Na}(\text{dca})$ (1 mmol) in 5 mL of H_2O to 1,10-phenanthroline (0.50 mmol) in 10 mL of ethanol. After being stirring for 4 h, the reaction mixture was filtered, and the filtrate was kept at room temperature. Prismatic single crystals suitable for X-ray analyses were obtained by slow evaporation of the solvent after a few days. Yield: 79.8% (based on Pr) for **1**; 75.7% (based on Gd) for **2**; 73.5% (based on Sm) for **3**. IR (KBr): 2283 (m), 2262 (m), 2225 (m), 2217 (m), 2154 (vs), 1519 (w), 1425 (m), 1346 (w), 1322 (w), 848 (m), 838 (m), 729 (s) for **1**; 2285 (m), 2262 (m), 2229 (m), 2217 (m), 2159 (vs), 1519 (w), 1423 (m), 1346 (w), 1322 (w), 850 (m), 839 (m), 730 (s) for **2**; 2283 (m), 2260 (m), 2219 (m), 2217 (m), 2156 (vs), 1519 (w), 1421 (m), 1346 (w), 1321 (w), 1108 (w), 848 (m), 838 (m), 728 (s) for **3**. Anal. Calcd for **1**: C, 54.03; H, 3.24; N, 22.51%. Found: C, 54.01; H, 2.84; N, 22.62%. Anal. Calcd for **2**: C, 53.10; H, 3.18; N, 22.12%. Found: C, 53.21; H, 3.05; N, 22.48%. Anal. Calcd for **3**: C, 53.49; H, 3.20; N, 22.28%. Found: C, 53.21; H, 3.05; N, 22.48%.

Preparations of $[\text{Ln}(\text{dca})_3(2,2'\text{-bipy})_2(\text{H}_2\text{O})]_n$ (4–6**).** A mixture of reactants was obtained by adding $\text{Ln}(\text{ClO}_4)_3$ (1 M, 0.5 mL) and $\text{Na}(\text{dca})$ (3 mmol) in 5 mL of H_2O to 2,2'-bipy (0.50 mmol) in 10 mL of ethanol. After being stirring for 5 h, the reaction mixture was filtered, and the filtrate was kept at room temperature. Prism single crystals suitable for X-ray analyses were obtained by slow evaporation of the solvent after a few days. Yield: 56.3% (based on Gd) for **4**; 85.2% (based on Sm) for **5**; 58.8% (based on La) for **6**. IR (KBr): 2294 (s), 2230 (s), 2161 (vs), 1598 (m), 1475 (w), 1435 (s), 1368 (m), 1010 (w), 759 (m) for **4**; 2293 (s), 2231 (s), 2173 (vs), 1598 (m), 1475 (w), 1435 (s), 1367 (m), 1010 (w), 759 (m) for **5**; 2300 (s), 2230 (s), 2164 (vs), 1598 (m), 1475 (w), 1434 (s), 1367 (m), 1009 (w), 759 (m) for **6**.

X-ray Crystallographic Studies. The crystal structures of six complexes were studied by single-crystal X-ray diffraction analyses. Data collections were performed at 293(2) K on a Rigaku Mercury CCD diffractometer for **1, 2, and 4–6**, on Siemens SMART CCD diffractometer for **3** with graphite monochromatic $\text{Mo K}\alpha$ radiation ($\lambda = 0.71073$ Å). The CrystalClear software⁹ was used for data reduction and empirical absorption correction for **1, 2, and 4–6**. For **3**, Siemens SAINT¹⁰ software was used for data reduction and empirical absorption corrections SADABS¹¹ based on measurements

- (4) (a) Escuer, A.; Mautner, F. A.; Sanz, N.; Vicente, R. *Inorg. Chem.* **2000**, *39*, 1668. (b) Manson, J. L.; Arif, A. M.; Incarvito, C. D.; Liable-Sands, L. M.; Rheingold, A. L.; Miller, J. S. *J. Solid State Chem.* **1999**, *145*, 369. (c) Marshall, S. R.; Incarvito, C. D.; Shum, W. W.; Rheingold, A. L.; Miller, J. S. *Chem. Commun.* **2002**, 3006. (d) Vangdal, B.; Carranza, J.; Lloret, F.; Julve, M.; Sletten, J. *J. Chem. Soc., Dalton Trans.* **2002**, 566. (e) Shi, Y. J.; Chen, X. T.; Li, Y. Z.; Xue, Z. L.; You, X. Z. *New J. Chem.* **2002**, *26*, 1711.
- (5) (a) Batten, S. R.; Jensen, P.; Moubaraki, B.; Murray, K. S.; Robson, R. *Chem. Commun.* **1998**, 439. (b) Kurmoo, M.; Kepert, C. J. *New J. Chem.* **1998**, 1515. (c) Manson, J. L.; Kmetz, C. R.; Epstein, A. J.; Miller, J. S. *Inorg. Chem.* **1999**, *38*, 2552. (d) Batten, S. R.; Jensen, P.; Kepert, C. J.; Kurmoo, M.; Moubaraki, B.; Murray, K. S.; Price, D. J. *J. Chem. Soc., Dalton Trans.* **1999**, 2987. (e) Jensen, P.; Batten, S. R.; Fallon, G. D.; Moubaraki, B.; Murray, K. S.; Price, D. J. *Chem. Commun.* **1999**, 177. (f) Manson, J. L.; Lee, D. W.; Rheingold, A. L.; Miller, J. S. *Inorg. Chem.* **1998**, *37*, 5966. (g) Britton, D. *Acta Crystallogr. Sect. C* **1990**, *46*, 2297.
- (6) (a) Marshall, S. R.; Incarvito, C. D.; Manson, J. L.; Rheingold, A. L.; Miller, J. S. *Inorg. Chem.* **2000**, *39*, 1969. (b) Sun, B. W.; Gao, S.; Ma, B. Q.; Wang, Z. M. *New J. Chem.* **2000**, *24*, 953. (c) Riggio, I.; van Albada, G. A.; Ellis, D. D.; Spek, A. L.; Reedijk, J. *Inorg. Chim. Acta* **2001**, *313*, 120. (d) Martin, S.; Barandika, M. G.; Ruiz de Larramendi, J. I.; Cortes, R.; Font-Bardia, M.; Lezama, L.; Serna, Z. E.; Solans, X.; Rojo, T. *Inorg. Chem.* **2001**, *40*, 3687. (e) Manson, J. L.; Huang, Q.-Z.; Lynn, J. W.; Koo, H. J.; Whangbo, M. H.; Bateman, R.; Otsuka, T.; Wada, N.; Argyriou, D. N.; Miller, J. S. *J. Am. Chem. Soc.* **2001**, *123*, 162. (f) Jensen, P.; Batten, S. R.; Moubaraki, B.; Murray, K. S. *J. Solid State Chem.* **2001**, *159*, 352. (g) Manson, J. L.; Incarvito, C. D.; Arif, A. M.; Rheingold, A. L.; Miller, J. S. *Mol. Cryst. Liq. Cryst. Sci. Technol., Sect. A* **1999**, *334*, 605. (h) Manson, J. L.; Incarvito, C. D.; Rheingold, A. L.; Miller, J. S. *J. Chem. Soc., Dalton Trans.* **1998**, 3705. (i) Potocnak, I.; Dunaj-Jurco, M.; Miklos, D.; Kabesova, M.; Jager, L. *Acta Crystallogr., Sect. C* **1995**, *51*, 600. (j) Wang, Z. M.; Luo, J.; Sun, B. W.; Yan, C. H.; Liao, C. S.; Gao, S. *Acta Crystallogr., Sect. C* **2000**, *56*, e242. (k) Wang, Z. M.; Luo, J.; Sun, B. W.; Yan, C. H.; Gao, S.; Liao, C. S. *Acta Crystallogr., Sect. C* **2000**, *56*, 786. (l) Luo, J. H.; Hong, M. C.; Weng, J. B.; Zhao, Y. J.; Cao, R. *Inorg. Chim. Acta* **2002**, *329*, 59. (m) Jensen, P.; Batten, S. R.; Moubaraki, B.; Murray, K. S. *Chem. Commun.* **2000**, 793. (n) Kutasi, A. M.; Batten, S. R.; Moubaraki, B.; Murray, K. S. *J. Chem. Soc., Dalton* **2002**, 819. (o) Jensen, P.; Price, D. J.; Batten, S. R.; Moubaraki, B.; Murray, K. S. *Chem. Eur. J.* **2000**, *6*, 3186. (p) Sun, H. L.; Gao, S.; Ma, B. Q.; Su, G. *Inorg. Chem.* **2003**, *42*, 5399.
- (7) (a) Skopenko, V. V.; Kapshuk, A. O.; Kramareuko, F. G. *Dop. Akad. Nauk. Ukr. RSR, Ser. B-Fiz.-Mat. Nauki* **1982**, *73*. (b) Kapshuk, A. A.; Skopenko, V. V. *Koord. Khim.* **1986**, *12*, 380.
- (8) (a) Wu, A. Q.; Zheng, F. K.; Cai, L. Z.; Guo, G. C.; Mao, J. G.; Huang, J. S. *Acta Crystallogr., Sect. E* **2003**, *59*, m257. (b) Wu, A. Q.; Cai, L. Z.; Chen, W. T.; Guo, G. C.; Huang, J. S. *Acta Crystallogr., Sect. C* **2003**, *59*, m491.

(9) Rigaku, CrystalClear 1.35, Software User's Guide for the Rigaku R-Axis, and Mercury and Jupiter CCD Automated X-ray Imaging System; Rigaku Molecular Structure Corporation: Utah, 2002.

Table 1. Crystal Data and Structure Refinement for the Complexes 1–3

complex	[Pr(dca) ₂ (Phen) ₂ (H ₂ O) ₃]- (dca)·(phen) (1)	[Gd(dca) ₂ (Phen) ₂ (H ₂ O) ₃]- (dca)·(phen) (2)	[Sm(dca) ₂ (Phen) ₂ (H ₂ O) ₃]- (dca)·(phen) (3)
formula	C ₄₂ H ₃₀ OPrN ₁₅ O ₃	C ₄₂ H ₃₀ GdN ₁₅ O ₃	C ₄₂ H ₃₀ SmN ₁₅ O ₃
fw	933.72	950.06	943.16
space group	<i>P2₁/n</i>	<i>P2₁/n</i>	<i>P2₁/n</i>
<i>a</i> (Å)	14.272 (4)	14.206 (4)	14.2073(1)
<i>b</i> (Å)	16.596(5)	16.462(3)	16.6396(3)
<i>c</i> (Å)	17.282(5)	17.217(3)	17.2861(4)
β (°)	91.094(4)	91.12 (2)	91.211(1)
<i>V</i> (Å ³)	4093(2)	4025.6(15)	4085.59(12)
<i>Z</i>	4	4	4
ρ (g/cm ³)	1.515	1.568	1.533
μ (mm ⁻¹)	1.250	1.708	1.497
λ (Å)	0.71073	0.71073	0.71073
<i>T</i> (K)	293(2)	293(2)	293(2)
<i>R</i> ₁ , <i>wR</i> ₂ (obsd)	0.0380, 0.0813	0.0407, 0.1088	0.0668, 0.1552
GOF	1.051	1.046	1.072
largest and mean δ/σ	0.006, 0.000	0.004, 0.000	0.001, 0.000
largest difference peak (e ⁻ Å ⁻³)	0.588, -0.519	1.194, -1.221	1.412, -0.998

Table 2. Crystal Data and Structure Refinement for Complexes 4–6

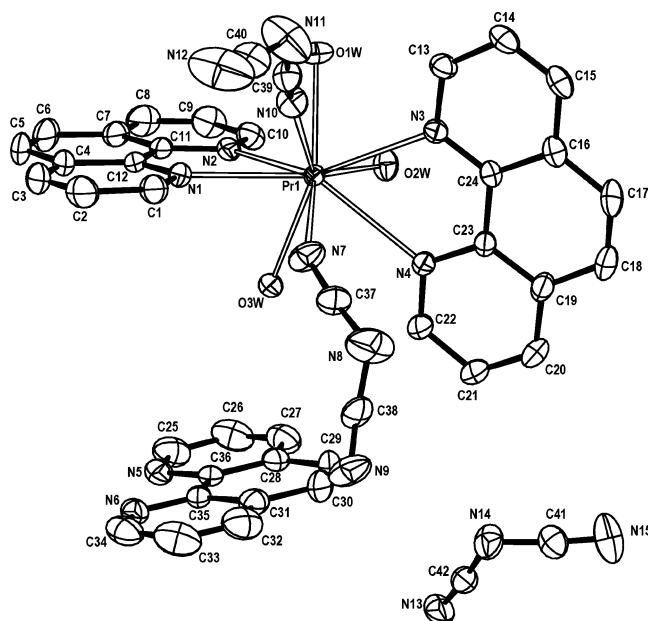
complex	[Gd(dca) ₃ (2,2'-bipy) ₂ (H ₂ O)]: (4)	[Sm(dca) ₃ (2,2'-bipy) ₂ (H ₂ O)]: (5)	[La(dca) ₃ (2,2'-bipy) ₂ (H ₂ O)]: (7)
formula	C ₂₆ H ₁₈ GdN ₁₃ O	C ₂₆ H ₁₈ SmN ₁₃ O	C ₂₆ H ₁₈ LaN ₁₃ O
fw	685.78	678.88	667.44
space group	<i>Pnna</i>	<i>Pnna</i>	<i>Pnna</i>
<i>a</i> (Å)	11.3940(10)	11.378(2)	11.2806(6)
<i>b</i> (Å)	15.5392(11)	15.625(3)	15.8467(9)
<i>c</i> (Å)	15.9601(12)	16.048(3)	16.1837(10)
<i>V</i> (Å ³)	2825.8(4)	2853.0(10)	2893.0(3)
<i>Z</i>	4	4	4
ρ (g/cm ³)	1.617	1.581	1.532
μ (mm ⁻¹)	2.392	2.103	1.521
λ (Å)	0.71073	0.71073	0.71073
<i>T</i> (K)	293(2)	293(2)	293(2)
<i>R</i> ₁ , <i>wR</i> ₂ (obsd)	0.0334, 0.0698	0.0422, 0.1078	0.0540, 0.1888
GOF	1.017	1.054	1.077
largest and mean δ/σ	0.000, 0.000	0.002, 0.000	0.001, 0.000
largest difference peak (e ⁻ Å ⁻³)	1.182, -0.511	1.921, -1.091	1.373, -0.691

of equivalent reflections used. The structures were solved by direct methods, which revealed the positions of the metal atoms using Siemens SHELXTL Version 5.0 package of crystallographic software.¹² The remaining non-hydrogen atoms were located by successive different Fourier syntheses. All hydrogen atoms were calculated in idealized positions and allowed to ride on their parent atom except for water molecules. The structures were refined using full-matrix least-squares refinement on F^2 . All non-hydrogen atoms were refined anisotropically. Pertinent crystal data and structure refinement results for six complexes are listed in Tables 1 and 2.

Results and Discussion

Description of the Structures. The X-ray crystallography revealed that 1–3 and 4–6 are isomorphous, respectively, so we will choose 1 and 4 to represent two series for detailed structural discussions.

[Ln(dca)₂(Phen)₂(H₂O)₃](dca)·(phen). The molecular unit of 1 is mononuclear consisting of discrete [Pr(dca)₂(Phen)₂(H₂O)₃]⁺ cations, dca anions, and lattice phen molecule, as shown in Figure 1. The Pr atom is coordinated by two terminal N atoms from two different dca ligands, four N atoms from two chelating phen molecules, and three water

**Figure 1.** ORTEP drawing of complex 1 with thermal ellipse at the 30% probability level with the hydrogen atoms being omitted for clarity.

molecules. These nine coordination atoms form a distorted tricapped trigonal prism. One of the trigonal faces is defined by one nitrogen atom from one phen ligand and two water oxygen atoms [N3, O1W, and O2W]; the other one is defined by one nitrogen atom from the other crystallographically

- (10) Siemens, SAINT Software Reference Manual; Siemens Energy & Automation Inc.: Madison, WI, 1994.
 (11) Sheldrick, G. M. *SADABS*, Absorption Correction Program; University of Goettingen: Goettingen, Germany, 1996.
 (12) Siemens. *SHELXTL*, Version 5.0, Reference Manual; Siemens Analytical X-ray Instruments Inc.; Madison, WI, 1995.

unique phen ligand, one terminal nitrogen atom from the other crystallographically unique dca ligand, and one oxygen atom of the third water molecule [N1, N7, and O3W]. Each square face is capped by two other nitrogen atoms from two phen ligands and one terminal nitrogen atom from the other dca [N2, N4, and N10]. The Pr(III) atom locates in the plane defined by the three capping atoms with the deviation of 0.037 Å from this plane in the direction toward the plane defined by the atoms of N1, N5, and O3W. The bond angles N(cap)–Pr–N(cap) are 129.43(5)° for N2–Pr1–N4, 113.74(5)° for N2–Pr1–N10, and 116.77(6)° for N4–Pr1–N10, respectively, which are close to 120° in a regular triangle. The bond lengths of the Pr(III) atom coordinated to the N atoms of phen ligands (Pr1–N1 = 2.676(2), Pr1–N2 = 2.713(2), Pr1–N3 = 2.702(2), Pr1–N4 = 2.756(2) Å with an average distance of 2.712(2) Å) are comparable to those of the Pr(III) analogue with the phen ligands¹³ but are distinctly longer than those of Pr(III) coordinated to nitrile N atoms of dca ligands (Pr1–N7 = 2.573(2), Pr1–N10 = 2.551(2) Å with the mean distance of 2.562(2) Å) due to the steric effect of the large phen molecules. The Pr1–O(water) bond distances (Pr1–O1W = 2.478(2), Pr1–O2W = 2.481(1), Pr1–O3W = 2.495(1) Å) are consistent with the typical distances of Ln(III)–O(water) bonds.¹⁴ In **1–3**, the Ln–N(phen) and Ln–O(water) bond lengths become shorter with the increase of the atom number of Ln due to the lanthanide contraction except for Ln–N(dca) bond distances.

The dca ligands are terminally coordinated with only one of the nitrile nitrogens involved in the bonding interactions with the metal atoms Ln(III). The coordinated dca ligands have pseudo C_{2v} symmetry with average C–N and N≡C bond length of 1.296(4) and 1.118(4) Å, respectively, which are slightly longer and shorter than those of commonly observed in dca anions (C–N = 1.270 Å, N≡C = 1.153 Å),¹⁵ respectively. The uncoordinated dca ligand has also pseudo C_{2v} symmetry with average C–N and N≡C bond lengths of 1.299(3) and 1.136(3) Å, which are comparable with those of the coordinated dca. In the coordinated dca anions the N≡C–N bond angles (N7–C37–N8 = 173.3(3), N8–C38–N9 = 172.8(3), N10–C39–N11 = 173.1(3), and N11–C40–N12 = 170.4(3)°) are almost linear while the C–N–C bond angles (C37–N8–C38 = 120.7(3), C39–N11–C40 = 121.7(3)°) are close to 120°. Each dca anions are in a planar geometry with the largest deviation of 0.014 Å from the mean plane for C38. The three crystallographically unique phen molecules are also almost coplanar with the largest deviation of atoms from the mean plane being 0.046 Å for C21. The two crystallographically unique coordinated phen ligands are almost perpendicular to each other with the dihedral angle of 84.16(3)° and located at the opposite sides of the Pr atom.

(13) Pisarevsky, A. P.; Mitrofanova, N. D. Frolovskaya, S. N. Martynenko, L. I. *Koord. Khim.* **1995**, *21*, 944.

(14) Piro, O. E.; Castellano, E. E.; Baran, E. J. Z. *Anorg. Allg. Chem.* **2002**, *628*, 612.

(15) Potocnak, I.; Duanj-Jurco, M.; Miklos, D.; Jager, L. *Jager. Acta Crystal. Sect. C* **1996**, *52*, 1653.

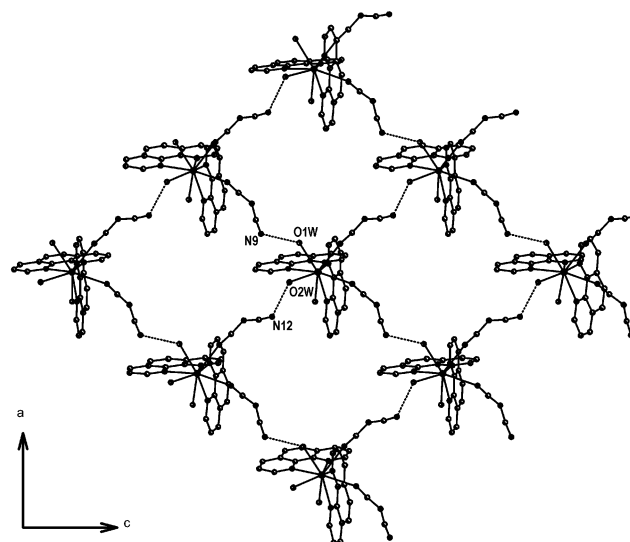


Figure 2. 2D (4,4) cationic layer structure of complex **1** is formed through hydrogen bond interactions; the hydrogen bonds represented by dotted lines.

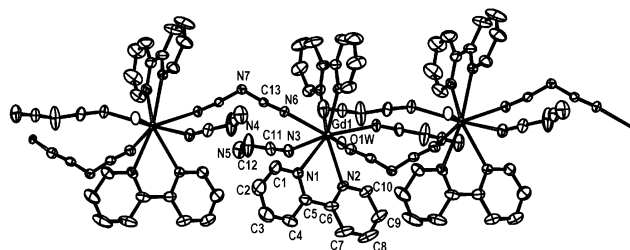


Figure 3. Chain structure of complex **4** with thermal ellipse at the 30% probability level extended along the *b* direction. The hydrogen atoms being omitted for clarity.

Extensive intermolecular hydrogen bonds are also observed in the crystal structures of **1–3**. The Pr(III) coordination unit in **1** is linked by O2W···N12 hydrogen bonds with the distance of 2.757(3) Å to form a chain along the [101] direction, and the chains synchronously form a layerlike structure by O1W···N9 hydrogen bonds with the distance of 2.796(3) Å along the [101] direction, as shown in Figure 2. The cationic layer constructed by hydrogen bonds may be considered as a noninterpenetrated 2D (4,4) network.¹⁶ The closest Pr···Pr separation bridged by the hydrogen bonding interactions is 11.102 Å. The uncoordinated dca anions bridge the layers to form a three-dimensional framework via O–H···N hydrogen bonds (O1W···N13 = 2.731(2), O2W···N15 = 2.717(3) Å) along the *b* axis, in which the lattice phen molecules are located with their N atoms hydrogen-bonding to O3W water molecules (O3W···N5 = 2.835(2), O3W···N6 = 2.771(2) Å).

[Ln(dca)₃(2,2'-bipy)₂(H₂O)]_n. Figure 3 shows the chain-like structure of complex **4**. The Gd(III) atom, residing at 4d position, is in a distorted tricapped trigonal prism environment with four nitrile N atoms from four different dca ligands, four N atoms from two chelating 2,2'-bipy molecules, and one water molecule. The trigonal faces are both defined by two N atoms of dca ligands and one nitrogen atom of 2,2'-bipy ligand [N2, N3, and N6 for both faces],

(16) Batten, S. R.; Robson, R. *Angew. Chem., Int. Ed.* **1998**, *37*, 1460.

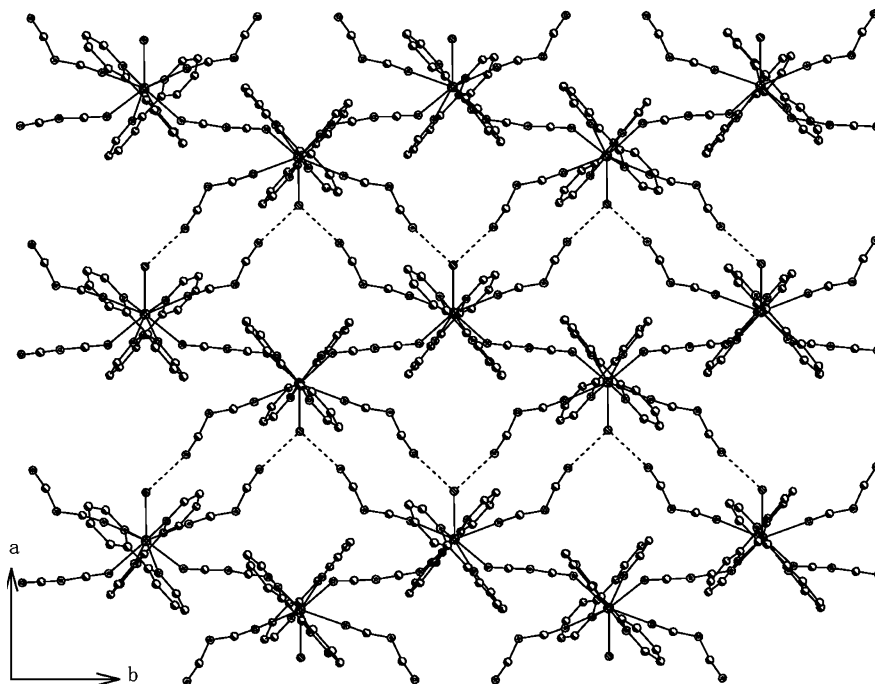


Figure 4. Layer structure of complex **4** is formed through O1W...N5 hydrogen bond interactions; the hydrogen bonds represented by dotted lines.

while the three capping positions are occupied by the remaining coordinated atoms [two N1 and one O1W atoms] with coplane with Gd atom. The bond angles $N_{(\text{cap})}-\text{Gd}-N(\text{O})_{(\text{cap})}$ range from $116.92(17)^\circ$ to $121.54(8)^\circ$, which are close to 120° in a regular triangle. The coordination modes of dca ligands in **4–6** can be classified as two types of bridging and terminal ligands. The bridging $[\text{N}(\text{CN})_2]^-$ ligands end-to-end link the Gd(III) atoms to form infinite chain extended along the *b* axis; the 2,2'-bipy ligands chelated to Gd(III) atoms are located on the both side of the chain. The closest intrachain Gd(III)...Gd(III) separation is 8.528 Å, which is shorter than the Ln(III)...Ln(III) distance of **1**. The bond lengths of the Gd(III) atom coordinated to the N atoms of 2,2'-bipy ligands (Gd1–N1 = 2.669(3), Gd1–N2 = 2.606(3) Å) are also distinctly longer than those of Gd(III) coordinated to nitrile N atoms of dca ligands (Gd–N3 = 2.481(4), Gd–N6 = 2.492(3) Å) as in the case found in the first series. The Ln–N(O) bond lengths in **4–6** become shorter with the increase of the atom number of Ln due to the lanthanide contraction. The chains of complex **4** are linked by O1W...N5 hydrogen bonds with the distance of 2.790(6) Å to form layerlike structure along the *a* and *b* directions, as shown in Figure 4.

The structures of the first series consisting of discrete complex units are different from that of the second series with infinite chainlike structure. The difference between these two series complexes is the size of ancillary ligands, which is the major factor on the architecture of molecular structures. The Ln–N(bipy) (the average Gd1–N(bipy) lengths in **4** is 2.637(3) Å and the average Sm1–N(bipy) lengths in **5** is 2.663(2) Å) is thus shorter than the Ln–N(phen) (the average Gd1–N(phen) lengths in **2** is 2.654(2) Å and the average Sm1–N(phen) lengths in **3** is 2.671(3) Å). If using the smaller steric ancillary ligands, the extended array complexes

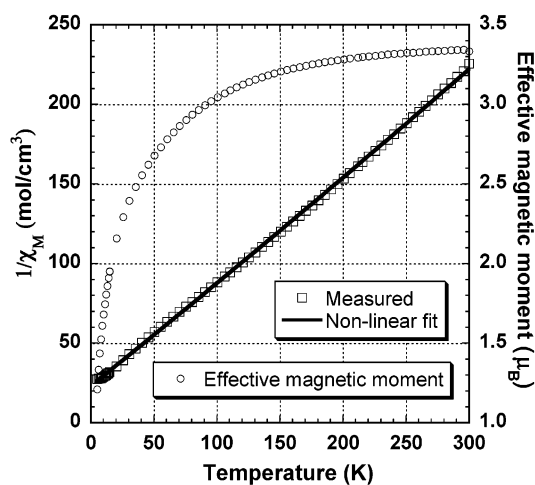


Figure 5. Plot of $1/\chi_M$ vs T over 5–300 K at a field of 1 T showing a Curie–Weiss paramagnetic behavior of complex **1** (Pr). The gradual but significant decrease of μ_{eff} upon cooling suggests the presence of anti-ferromagnetic interactions.

such as two- or three-dimensional structure may be expected. Further studies on this idea are in progress.

Magnetic Properties. The neutrality requirement for **1–6** suggests a formal oxidation state of +3 for lanthanide cations, which is confirmed by the temperature-dependent magnetic susceptibility measurements for **1**, **2**, **4**, and **5**. A $1/\chi_M$ – T plot in Figures 5 and 6 shows that the phases are paramagnetic over 5–300 K (χ_M is the magnetic susceptibility per Ln(III) ions). For **1** (Pr), a nonlinear fit via $\chi_M = C/(T - \theta) + \chi_0$ reveals a Curie–Weiss behavior with the Curie constant $C = 1.58(4) \text{ cm}^3 \text{ mol}^{-1} \text{ K}$, the Weiss constant $\theta = -36.1(9)^\circ$, and the background susceptibility, $\chi_0 = -2(1) \times 10^{-4} \text{ cm}^3/\text{mol}$. An effective magnetic moment of 3.57(5) μ_B can thus be obtained for each Pr center, which is close to the expected 3.58 μ_B for the free-ion ground state (3H_4) of Pr(III) with two localized unpaired f-electrons. For **2** (Gd),

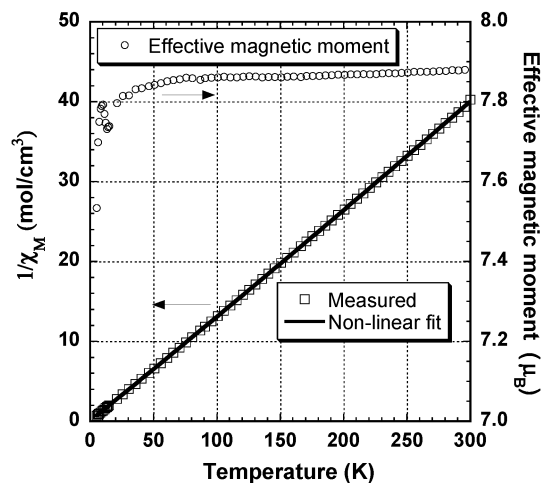


Figure 6. Plot of $1/\chi_M$ vs T over 5–300 K at a field of 1 T showing a Curie–Weiss paramagnetic behavior of complex **2** (Gd). The gradual decrease of μ_{eff} upon cooling suggests the presence of weak antiferromagnetic interactions.

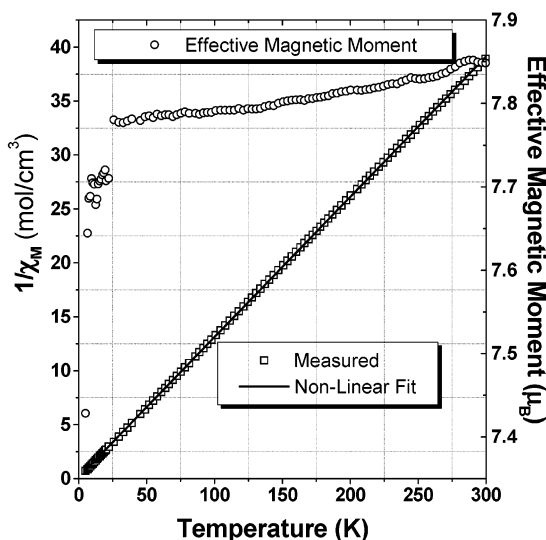


Figure 7. Plot of $1/\chi_M$ vs T over 5–300 K at a field of 1 T showing a Curie–Weiss paramagnetic behavior of complex **4** (Gd). The gradual decrease of μ_{eff} upon cooling suggests the presence of weak antiferromagnetic interactions.

a similar nonlinear fit to the data above 20 K shows a Curie–Weiss behavior with $C = 7.760(4) \text{ cm}^3 \text{ mol}^{-1} \text{ K}$, $\theta = -0.44(1)^\circ$, and $\chi_0 = -8.6(3) \times 10^{-4} \text{ cm}^3/\text{mol}$. Each Gd ion thus features an effective magnetic moment of $7.878(2) \mu_B$, which is close to the theoretical $7.94 \mu_B$ for the free-ion ground state ($^8S_{7/2}$) of Gd(III) with seven localized unpaired f-electrons.

The magnetic properties of **4** and **5** in the second series complexes in the form of $1/\chi_M$ versus T are shown in Figures 7 and 8, respectively. For **4** (Gd), a nonlinear fit via $\chi_M = C/(T - \theta) + \chi_0$ above 20 K reveals a Curie–Weiss behavior with $C = 7.65(2) \text{ cm}^3 \text{ mol}^{-1} \text{ K}$, $\theta = -0.47(7)^\circ$, and $\chi_0 = -9.4(1) \times 10^{-4} \text{ cm}^3/\text{mol}$. An effective magnetic moment of $7.82(1) \mu_B$ can thus be obtained for each Gd(III) center, which is close to the expected $7.94 \mu_B$ for the free-ion ground state ($^8S_{7/2}$) of Gd(III) with seven localized unpaired f-electrons. For **5** (Sm), a similar nonlinear fit to the data above 15 K shows a Curie–Weiss behavior with $C = 0.0856(6)$

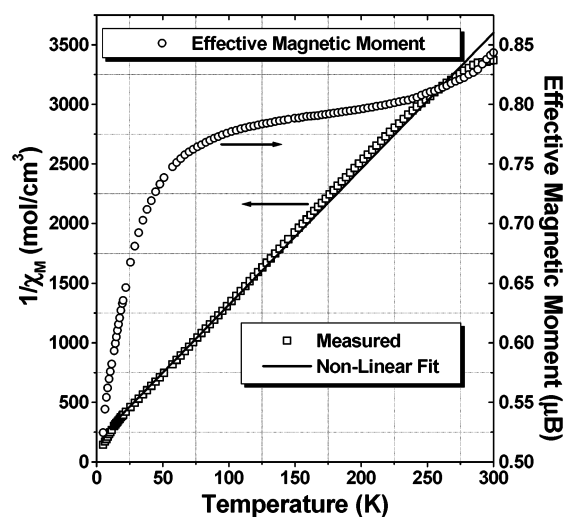


Figure 8. Plot of $1/\chi_M$ vs T over 5–300 K at a field of 1 T showing a Curie–Weiss paramagnetic behavior of complex **5** (Sm). The gradual decrease of μ_{eff} upon cooling suggests the presence of weak antiferromagnetic interactions.

$\text{cm}^3 \text{ mol}^{-1} \text{ K}$, $\theta = -13.6(3)^\circ$, and $\chi_0 = 4.40(3) \times 10^{-4} \text{ cm}^3/\text{mol}$. Each Sm(III) ion features an effective magnetic moment of $0.827(3) \mu_B$, which is close to the theoretical $0.84 \mu_B$ for the free-ion ground state ($^6H_{5/2}$) of Sm(III) with five localized unpaired f-electrons.

The decreases in the μ_{eff} values with decreasing temperature of complexes **1**, **2**, **4** and **5** indicate the presence of antiferromagnetic interactions among Ln(III) ions. This 4f–4f antiferromagnetic interaction is much smaller¹⁷ as compared with that between 3d metal ions or even between 4f and 3d ions.¹⁸ The magnetic behaviors of **2** and **4** with Gd(III) ions is basically similar, showing weak antiferromagnetic interactions in these two complexes, which is consistent with the previous report about the occurrence of an antiferromagnetic ground state in homopolynuclear gadolinium complexes¹⁹ but contradicts that reported by Costes et al. in 2002.²⁰ The origin for the small dip at ~ 13 K for **2** and **4** is still unclear but may be related to the splitting of the $^8S_{7/2}$ multiple at zero fields (ZFS) or to a weak antiferromagnetic interaction between neighboring molecules.²¹

(17) Panagiotopoulos, A.; Zafiropoulos, T. F.; Perlepes, S. P.; Bakalbassis, E.; Masson-Ramade, I.; Kahn, O.; Terzis, A.; Raptopoulou, C. P. *Inorg. Chem.* **1995**, *34*, 4918.

(18) (a) Benelli, C.; Fei, A.; Gatteschi, D.; Pardi, L. *Inorg. Chem.* **1988**, *27*, 2831. (b) Andruh, M.; Ramade, I.; Codjovi, E.; Guillou, O.; Kahn, O.; Trombe, J. C. *J. Am. Chem. Soc.* **1993**, *115*, 1822.

(19) (a) Panagiotopoulos, A.; Zafiropoulos, T. F.; Perlepes, S. P.; Bakalbassis, E.; Masson-Ramade, I.; Kahn, O.; Terzis, A.; Raptopoulou, C. P. *Inorg. Chem.* **1995**, *34*, 4918. (b) Hedinger, R.; Ghisletta, M.; Hegetschweiler, K.; Toth, E.; Merbach, A. E.; Sessoli, R.; Gatteschi, D.; Gramlich, V. *Inorg. Chem.* **1998**, *37*, 6698. (c) Costes, J. P.; Dahan, F.; Nicodème, F. *Inorg. Chem.* **2001**, *40*, 5285. (d) Liu, S.; Gelmini, L.; Rettig, S. J.; Thompson, R. C.; Orvig, C. *J. Am. Chem. Soc.* **1992**, *114*, 6081. (e) Guerriero, P.; Tamburini, S.; Vigato, P. A.; Benelli, C. *Inorg. Chim. Acta* **1991**, *189*, 19. (f) Costes, J. P.; Dupuis, A.; Laurent, J. P. *Inorg. Chim. Acta* **1998**, *268*, 125.

(20) Costes, J. P.; Clemente-Juan, J. M.; Dahan, F.; Nicodème, F.; Verelst, M. *Angew. Chem., Int. Ed.* **2002**, *41*, 323.

(21) Caneschi, A.; Dei, A.; Gatteschi, D.; Sorace, L.; Vostrikova, K. *Angew. Chem., Int. Ed.* **2000**, *39*, 246.

Concluding Remarks

In summary, we have reported the syntheses of two series novel rare earth complexes containing dca ligands. These complexes have all been structurally characterized by X-ray crystallography. The Ln(III) atoms have a typical 9-fold coordination with a distorted tricapped trigonal prism. The three-dimensional frameworks are constructed by intermolecular hydrogen bond interactions. Complexes **1**, **2**, **4**, and **5** follow the Curie–Weiss paramagnetic behavior down to 5 K.

Acknowledgment. This work was financially supported by the National Natural Science Foundation of China (20001007, 20131020), Natural Sciences Foundation of the Chinese Academy of Sciences (KJCX2-H3), and Fujian Province (2000F006).

Supporting Information Available: Additional details of crystal structure determinations and tables. This material is available free of charge via the Internet at <http://pubs.acs.org>.

IC035470J